

# The effects of gas flow rate and annealing on the morphological properties of zinc oxide nanostructures thin film using chemical vapour deposition process

W.H. Khoo <sup>a, b</sup>, S.M. Sultan <sup>a, b, \*</sup>, M.Z. Sahdan <sup>c</sup>

<sup>a</sup> Computational Nanoelectronics Research Group (CONE), Universiti Teknologi Malaysia, 81310 UTM Johor Bahru, Johor, Malaysia

<sup>b</sup> Faculty of Electrical Engineering, Universiti Teknologi Malaysia, 81310 UTM Johor Bahru, Johor, Malaysia

<sup>c</sup> Microelectronics and Nanotechnology Shamsuddin Research Center (MiNT-SRC), Universiti Tun Hussein Onn Malaysia, 86400 Parit Raja, Batu Pahat, Johor, Malaysia

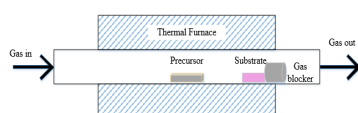
\* Corresponding author: suhanasultan@utm.my

## Article history

Received 25 May 2016

Accepted 20 December 2016

## Graphical abstract



## Abstract

Zinc Oxide nanostructures thin films have been deposited on glass substrates by using chemical vapour deposition technique at 1000°C assisted by gas blocker. Glass substrates was sputtered by ~5nm of gold to form a catalyst layer on top of glass. Different gas flow rates of 0.05, 0.10, 0.20, 0.40 L/min were used in the deposition. After the deposition, the layer was annealed at temperatures of 500°C for 1 hours under atmospheric pressure. The surface morphologies of ZnO thin film were investigated field emission scanning electron microscope (FESEM). X-ray diffraction (XRD) results confirm the presence of ZnO layer with high peak of (002) crystal orientation and shows improvement after annealing. The mechanism of ZnO nanostructures formation will be discussed in this paper.

**Keywords:** ZnO nanostructures, Chemical vapour deposition (CVD), Gas flow rate, Annealing

© 2017 Penerbit UTM Press. All rights reserved

## INTRODUCTION

Zinc Oxide (ZnO) is n-type group II-VI semiconductor crystallize in either cubic zinc-blende or hexagonal wurtzite structure where each anion is surrounded by four cations at the corners of a tetrahedron, and vice versa [1]. In addition, ZnO is a direct wide band-gap (3.37 eV) semiconductor with a large exciton binding energy (60 meV) and high thermal stability, making it an important semiconductor with wide applications in optoelectronics [2], solar cell [3], piezoelectric device [4] and gas sensing [5,6]. ZnO thin films can be prepared by using various methods including physical deposition or wet process. Some of the methods reported are sol-gel[7,8], pulsed-laser deposition [9,10], sputtering [11,12], spray pyrolysis, molecular beam deposition and chemical vapour deposition [13-15].

Chemical vapour deposition (CVD) is very attractive as a simple cost-effective means of preparing ZnO nanostructure. It is known that the growth of ZnO nanowires via CVD is sensitive to process conditions. Subtle changes in experimental conditions, such as source temperature, the distance between substrate and source, gas flow rate, substrate material, and choice of catalyst, can cause dramatic changes in the shape, density and size of the grown nanostructures. Therefore, it is important to investigate the parameters controlling the nanowires growth and the effect of these parameters on the ZnO nanowire structures. In this paper, we focus on the oxygen gas flow and the effect of annealing.

## EXPERIMENTAL

Figure 1 shows the thermal CVD system which consists of the thermal furnace, a gas blocker, Argon and Oxygen gas flow, alumina boat used to put precursor and alumina tube. Figure 2 shows the process flow of the fabrication process of ZnO thin film nanostructures. It starts with preparation of 2 cm x 2 cm glass substrate. The substrate was cleaned with acetone and ethanol using ultrasonic machine respectively for 10 minutes, then cleaned with deionized water and dried with nitrogen gas. About 5nm of gold was coated on the cleaned glass.

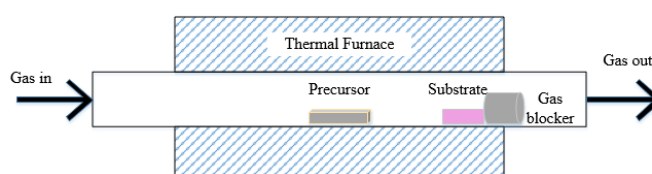


Fig. 1 The schematic diagram of thermal CVD system.

The sample was put inside the CVD chamber under low pressure and temperature for ZnO nanostructure thin film deposition. After deposition, the samples were characterized in XRD to confirm the presence of zinc oxide peaks. The morphologies of thin film was observed using field emission scanning electron microscopy (FESEM).

The whole process was repeated and optimized until ZnO nanostructures was deposited on glass substrate. The sample was then annealed at 500 °C in atmospheric environment for 1 hour. Figure 3 shows the processes involved against time during the CVD deposition. Initially, the furnace was kept at 27°C and 0.2 l/min of Ar gas flow was introduced for 10 min. Then, furnace temperature was ramped up at 20°C per minute until a maximum temperature of 1000°C was reached. The furnace was kept at 1000°C for 1 hour. During this time, the oxygen gas was fed in. Next, the chamber was cooled down to 100°C.

half maximum (FWHM) value. From the parameters obtained, the grain size of ZnO could be estimated using Scherer's formula as shows in equation [16]:

$$D = \frac{0.9\lambda}{B \cos\theta} \quad (1)$$

where D is grain size, λ is X-ray wavelength of 1.54 Å, B is FWHM of the XRD peaks in radian and θ is diffraction angle.

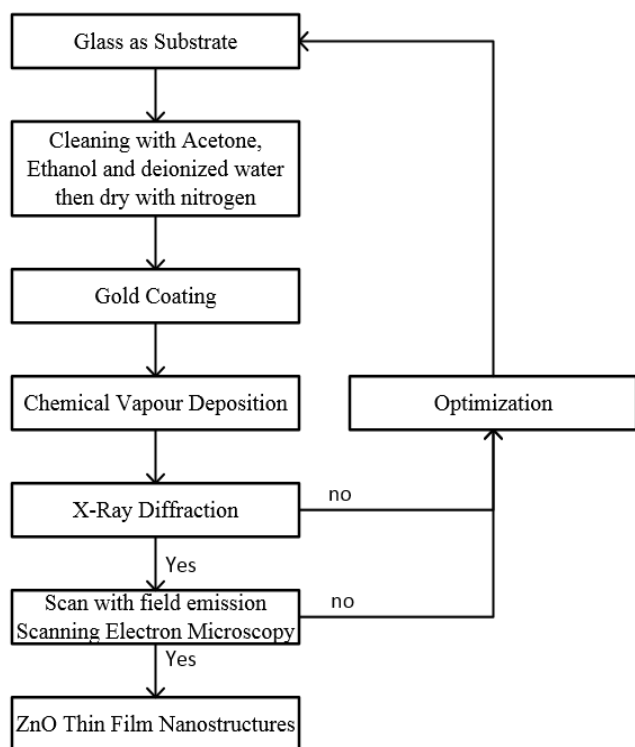


Fig.2 Fabrication Process flow.

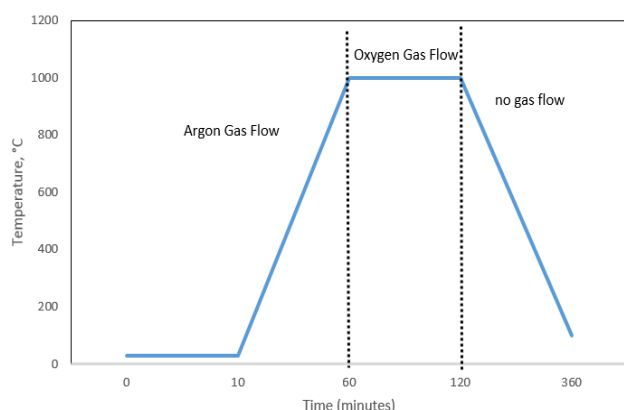


Fig. 3 Temperature versus time graph during CVD process.

## RESULTS AND DISCUSSION

Figure 4(a) shows the scanning electron image of amorphous ZnO nanostructure with oxygen gas flow of 0.05 l/min. The average grain size increases when oxygen gas flow increased to 0.4 l/min as shown in Figure 4(b).

Figure 5 shows the XRD pattern of ZnO thin film with different oxygen gas flow rate. From the spectrum, the main crystal orientation of ZnO thin film is along (0 0 2) and (1 0 1) at 34.37° and 36.36° respectively. Other orientations corresponding to (1 0 0) are present at 31.7°. The crystallinity improvement for all orientations is observed after annealing process. This is shown by the increment of full width at

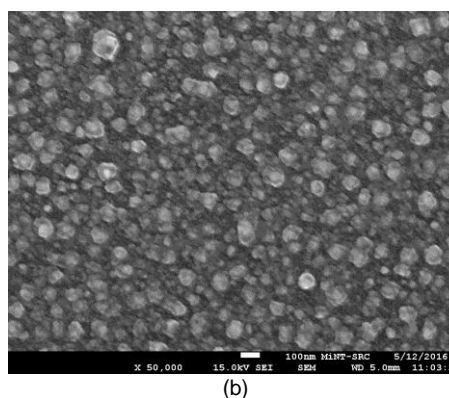
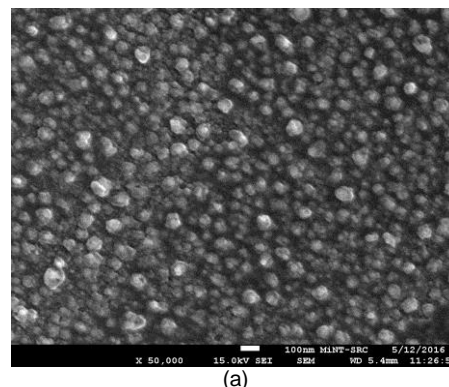


Fig 4 SEM image of ZnO nanostructure with oxygen gas flow of (a) 0.05 l/min. (b) 0.40 l/min.

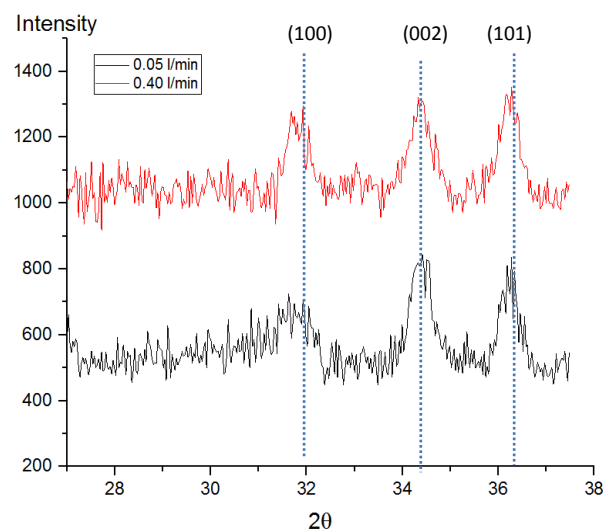


Fig. 5 XRD patterns of ZnO thin film with different oxygen gas flow.

Table 1 and Table 2 show the FWHM and grain sizes obtained before and after annealing for oxygen gas flow of 0.05 l/min and 0.40 l/min, respectively. For 0.05 l/min, the calculated grain size increases from 13.2 nm to 19.8 nm for (1 0 0) orientation, 22.9 nm to 26.9 nm for (0 0 2) orientation and highest increment for (1 0 1) orientation which increased by 12.5 nm after annealing process This increment might due

to the merging activity of the ZnO particles to form denser film after annealing with high temperature [17]. Meanwhile, the grain size and FWHM for ZnO thin film with oxygen flow rate of 0.40 l/min decreases after annealing. This might be due to the presence of more oxygen atoms surrounding Zn ions to form a weak and unstable bond when oxygen flow rate increases. After annealing, both ZnO thin films deposited with different flow rates show almost similar FWHM and grain size. This shows that the weak and unstable bond could be easily broken during annealing and atoms rearrange themselves to form a stable ZnO compound.

**Table 1** FWHM and grain size before and after annealing for ZnO thin film deposited at O<sub>2</sub> gas flow of 0.05 l/min

Lattice (h k l)	Before annealing		After annealing	
	FWHM	Grain size (nm)	FWHM	Grain size (nm)
1 0 0	0.71	13.20	0.47	19.89
0 0 2	0.41	22.96	0.35	26.90
1 0 1	0.47	20.13	0.30	32.68

**Table 2** FWHM and grain size before and after annealing for ZnO thin film deposited at O<sub>2</sub> gas flow of 0.4 l/min

Lattice (h k l)	Before annealing		After annealing	
	FWHM	Grain size (nm)	FWHM	Grain size (nm)
1 0 0	0.30	32.30	0.59	15.86
0 0 2	0.24	41.20	0.35	26.90
1 0 1	0.35	27.00	0.35	27.03

## CONCLUSION

Zinc oxide thin film nanostructure was successfully fabricated by thermal chemical vapour deposition. The grain size of the nanostructure during 0.05 l/min of oxygen flow shows smaller grain size compared to film deposited at 0.4 l/min. For 0.05 l/min, the grain sizes increase after annealing. However, for 0.4 l/min, the grain sizes reduce due to many dangling bonds present on the film before the annealing process. Therefore, FWHM from the XRD peaks and grain sizes change after annealing due to atoms rearranging themselves into stable form.

## ACKNOWLEDGEMENT

This work was supported by Ministry of Education Malaysia through Fundamental Research Grant Scheme (FRGS) vot 4F482. The authors would like to acknowledge the fabrication and experimental support from MiNT-SRC, Universiti Tun Hussein Onn Malaysia. The authors also acknowledge the support from UTM Research Management Centre.

## REFERENCES

- [1] A. K-Radzimska, T. Jesionowski, *Materials* 7 (2014) 2833-2881.
- [2] H. Wan, H.E. Ruda, *J. Mater. Sci.: Mater. Electron* 21 (2010) 1014-1019.
- [3] T. Yang, W. Cai, D. Qin, E. Wang, L. Lan, X. Gong, J. Peng, and Y. Cao., *J. Phys. Chem. C* 114 (2010) 6849-6853.
- [4] V.S. Nguyen, D. Rouxel, B. Vincent, L. Badie, F.D.D. Santos, E. Lamouroux, and Y. Fort, *Appl. Surf. Sci.* 279 (2013) 204-211.
- [5] J. Zhao, S. Wu, J. Liu, H. Liu, S. Gong, and D. Zhou, *Sensor Actuat. B: Chem.* 145 (2010) 788-793.
- [6] H.D. Setiabudi, A.A. Jalil, S. Triwahyono, N.H.N. Kamarudin, R.R. Mukti, *Appl. Catal. A: Gen.* 417-418 (2012) 190-199.
- [7] K. Ebitani, J. Konishi, H. Hattori, *J. Catal.* 130 (1991) 257-267.
- [8] T. Shishido, H. Hattori, *Appl. Catal. A: Gen.* 146 (1996) 157-164.
- [9] S. Triwahyono, T. Yamada, H. Hattori, *Catal. Lett.* 85 (2003) 109-115.
- [10] S. Triwahyono, Z. Abdullah, A.A. Jalil, *J. Nat. Gas Chem.* 15 (2006) 247-252.
- [11] S. Triwahyono, T. Yamada, H. Hattori, *Appl. Catal. A: Gen.* 242 (2003) 101-109.
- [12] N.N. Ruslan, N.A. Fadzillah, A.H. Karim, A.A. Jalil, S. Triwahyono, *Appl. Catal. A: Gen.* 406 (2011) 102-112.
- [13] W.C. Conner, J.L. Falconer, *Chem. Rev.* 95 (1995) 759-788.
- [14] O.B. Yang, S.I. Woo, in: L. Guzzi, F. Solymosi, P. Tetenyi (Eds.), *New Frontiers in Catalysis, Proc. 10th Int. Cong. Catal.*, Budapest, Hungary, 19-24 July 1992, Elsevier Science Publishers B.V., Amsterdam, 1993, p. 671-680.
- [15] A.K. Aboul-Gheit, A.E. Awadallah, N.A.K. Aboul-Gheit, E.S.A. Solyman, M.A. Abdel-Aaty, *Appl. Catal. A: Gen.* 334 (2008) 304-310.
- [16] A. Jentys, R.R. Mukti, H. Tanaka, J.A. Lercher, *Microporous Mesoporous Mater.* 90 (2006) 284-292.
- [17] M.A.A. Aziz, N.H.N. Kamarudin, H.D. Setiabudi, H. Hamdan, A.A. Jalil, S. Triwahyono, *J. Nat. Gas Chem.* 21 (2012) 29-36.